High-frequency dielectric loss of Na β-alumina: Evidence for relaxation crossover

K. L. Ngai and U. Strom
Naval Research Laboratory, Washington, D.C. 20375-5000
(Received 14 December 1987; revised manuscript received 28 April 1988)

The ionic-conductivity (σ) and electric-modulus (M^*) data for melt-grown Na β-alumina in the 10^2-10^7-Hz frequency range have been previously interpreted with a formalism in which the decay of an observable, such as the time-dependent electric field in the sample, follows the ("fractional-exponential") form $\exp[(-t/\tau)^{1-n}]$, where $0<n<1$. Ionic-conductivity data for frequencies between 10^8 and 10^{11} Hz cannot be interpreted in terms of this formalism, but instead the ionic relaxation at high frequencies is consistent with a simple exponential (i.e., with $n=0$). These observations are in agreement with the predictions of a relaxation model in which the frequency ω_c, which defines the crossover from fractional to simple exponential relaxation, is included as an explicit parameter.

I. INTRODUCTION

The fast-ion conductor Na β-alumina exhibits a variety of unique dielectric, acoustic, and thermal properties which are very much like those observed in glasses and amorphous polymers.[1] This behavior has been attributed to the topological disorder induced by the non-stoichiometric Na^+-ion excess within the conduction planes of this "superionic" conductor. The disorder leads to a high density of two-level tunneling modes [i.e., two-level systems (TLS)] which dominate the low-temperature properties of this crystalline solid. At higher temperatures (>90 K), thermally activated ionic conduction involving the cooperative motion of ion pairs constitutes the major contribution to the dielectric loss.[2] For frequencies between 10^2 and 10^7 Hz, this loss has been interpreted[3] satisfactorily in terms of a formalism[4,5] in which the decay of an observable, such as the time-dependent electric field within a capacitor $E(t)$, is of the Kohlrausch[6] ("fractional-exponential" or "stretched-exponential") form, i.e., $E(t)=E(0)\exp[(-t/\tau)^{1-n}]$, where $0<n<1$. For Na β-alumina n is typically $\sim 0.5-0.6$ and slightly temperature dependent for $T>100$ K. The observed fractional exponential relaxation is commonly observed also for the low-frequency ($<10^8$ Hz) permanent dipolar dielectric relaxation in many disordered solids.[7,8]

At high frequencies ($>10^8$ Hz), the dielectric loss in disordered solids is generally dominated by disorder-induced coupling to phonons.[9,10] The phonon-related far-infrared dielectric loss in many polymers and glasses depends approximately quadratically on frequency and is generally much larger than the loss due to electronic or ionic relaxation effects.

For Na β-alumina, on the other hand, the dielectric loss which can be attributed to a phonon mechanism, exhibits a much stronger frequency dependence ($\sim\omega^4$) over the $10^{10}-10^{12}$-Hz range.[1,11] This leads to a much diminished phonon-loss contribution below 10^{11} Hz compared to many other disordered solids. Consequently, the contribution of competing relaxation loss processes, due to the tunneling (at low temperatures) or (at sufficiently high temperature) hopping motion of ions, dominates the high-frequency dielectric loss in this material. Na β-alumina, therefore, offers a unique possibility to study the frequency dependence of the dielectric loss due to ionic relaxation into the microwave range. Previously, such a study has been carried out for the low-temperature loss which is dominated by tunneling modes.[12,13] The microwave-loss data at higher temperatures (>100 K) have been available,[1] but have not been interpreted in detail in conjunction with the low-frequency ($<10^7$ Hz) results. A particularly striking feature of these data is a dramatic change in the frequency dependence of the dielectric loss in the 10^9-10^{10}-Hz range. This observation has not been heretofore explained in a satisfactory manner.

The purpose of the present paper is to reexamine the dielectric-loss data for Na β-alumina in order to establish a definitive link between the data in the 10^2-10^7-Hz region and the 10^9-10^{12}-Hz region. It will be shown that the distinct change in frequency dependence of the dielectric loss near $\sim 10^{10}$ Hz can be interpreted in terms of a fundamental change in the ion relaxation mechanism. It will also be shown that this "crossover" in ionic relaxation is not only exhibited in the frequency dependence of the dielectric loss, but also in the temperature dependence of the dc conductivity. We believe that the present interpretation of the dielectric-loss data for Na β-alumina is of potential interest for other solids with significant ionic- or electronic-relaxation-loss contributions.

The outline of the paper is as follows. The next section briefly summarizes the appropriate experimental observations and describes previous theoretical fits to these data. The relaxation model employed in this paper is described in Sec. III, and the application of this model to the dielectric loss data is discussed in Sec. IV. Other corroborating evidence, which supports the theoretical interpretation, is presented in Sec. V. The significant conclusions are summarized in the final section.

II. DIELECTRIC-LOSS DATA

It has been shown by Macedo, Moynihan, and coworkers[4,5] that the appropriate function to analyze the dielectric relaxation due to mobile carriers is the inverse complex permitivity $M^*=1/\epsilon^*$, known as the electric

modulus. For an ionic conductor $M^*(\omega)$ provides information about the dynamic aspects of ion motion in terms of the time decay of the electric charges on opposite sides of the sample. This variation of the charge is described by the time variation of the electric field $E(t)=E(0)\Phi(t)$. The electric modulus is expressed as[4,5,14,15]

$$M^*(\omega)=M_\infty\left[1+\int_0^\infty dt\,\exp(-i\omega t)d\Phi(t)/dt\right], \quad (1)$$

where M_∞ is the high-frequency limit of the real part of $M^*(\omega)$. Note also that $M^*=M'+iM''=1/\epsilon^*=1/(\epsilon'-i\epsilon'')$. The imaginary part ϵ'' of the complex permittivity ϵ^* is related to the real part of the conductivity by

$$\sigma=\epsilon_0\epsilon'', \quad (2)$$

where ϵ_0 is the permittivity of free space. The frequency dependence of ϵ', ϵ'', and σ can be calculated via

$$\epsilon'=M'/[(M')^2+(M'')^2] \quad (3)$$

and Eq. (2), where

$$\epsilon''=M''/[(M')^2+(M'')^2]. \quad (4)$$

The dc conductivity σ_{dc} is related to the average relaxation time $\langle\tau\rangle$ of the electric field by

$$\sigma_{dc}=\lim_{\omega\to 0}\sigma(\omega)=\epsilon_0/(M_\infty\langle\tau\rangle), \quad (5)$$

where $\langle\tau\rangle$ is given by

$$\langle\tau\rangle=\int_0^\infty\Phi(t)dt. \quad (6)$$

In an analysis[4,5,14,15] of the electric modulus data for glassy ionic conductors it was determined empirically that the optimum form for $\Phi(t)$ was the "fractional-exponential" (Kohlrausch) form

$$\Phi(t)=\exp[-(t/\tau^*)^{1-n}],\quad 0<n<1, \quad (7)$$

where τ^* is a characteristic relaxation time. For $n=0$, Eq. (7) reduces to a simple exponential decay. The two adjustable parameters in Eq. (7) τ^* and n determine, respectively, the position and the shape of the imaginary part of the electric modulus. We have previously presented fits[3] using the above formalism to the electric-modulus data of Almond and West[2] for Na β-alumina. The data were taken over a frequency range from 10^2 Hz to slightly less than 10^7 Hz for temperatures ranging from 92 to 141 K. In the left portion of Fig. 1 the data of Almond and West are replotted on a logarithmic scale for a temperature of 113 K. The excellent fit to experiment is demonstrated by comparison with the calculated curve for $T=113$ K, as shown by the solid line in Fig. 1. The parameters used to obtain this fit were $n=0.64$ and $\log_{10}\tau^*=4.93$.

At frequencies greater than 10^7 Hz the quantity that is measured is the imaginary part of the dielectric constant ϵ'' which is related to the conductivity by Eq. (2). On the right side of Fig. 2 are shown the previously published[10,11] high-frequency conductivity data for Na β-alumina at several different temperatures. Also shown in Fig. 2 are the electric-modulus data of Almond and West[2] (as in the left portion of Fig. 1), where ϵ'' was obtained from the measured values for M' and M'' and Eq. (4). Using the inverse relations, as given by Eq. (3) and (4), has also led to the determination of the 113-K microwave frequency points on the right-hand side of Fig. 1.

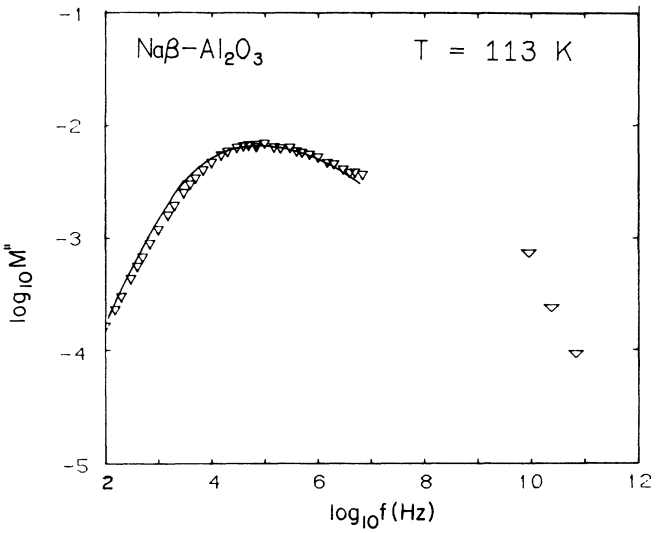

FIG. 1. Imaginary part of the electric modulus M'' data in a frequency range $10^2<f<10^{11}$ Hz at 113 K. The data in the low-frequency range of 10^2 to 10^7 Hz at 113 K are reproduced from data by Almond and West (Ref. 2).

The Kohlrausch-type fit to M'' in Fig. 1, when extended to frequencies higher than 10^7 Hz, predicts a frequency dependence[3] of M'' such that $\log_{10}M''\sim\omega^{n-1}$. On a log-log plot this implies a straight line with slope $n-1$, where $n\sim 0.65$. The measured microwave data clearly do not correspond to this prediction, but instead follow a curve predicted by $n=0$. The inability of the fractional exponential formalism[4,5] to explain the data above 10^7 Hz is demonstrated perhaps more succinctly in Fig. 2. Here the dependence of $\log_{10}\sigma\sim n\log_{10}f$, which is predicted

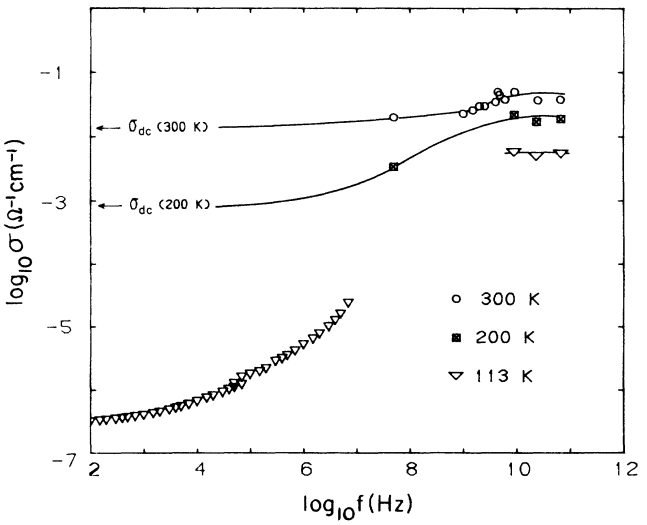

FIG. 2. ac conductivity data of Na β-alumina in the frequency range $10^2<f<10^{11}$ Hz for three different temperatures.

by Eq. (2) using Eqs. (1) and (4), is not displayed by the microwave data, which are independent of frequency at least over one decade in frequency near 10^{10} Hz.

III. RELAXATION MODEL

The empirical fractional exponential model[4,5] outlined by Eqs. (1)–(7) cannot account for all of the data shown in Figs. 1 and 2. An alternate model has been proposed[8,16–20] which contains some of the essential features of the empirical "fractional-exponential" model,[4,5] but also several additional parameters which can be directly related to microscopic observables. As will be seen, this "coupling" model leads to several coupled equations containing one set of parameters. A detailed outline of the model can be found elsewhere.[8,16–19] Some of the essential results will be given here. An important application of the coupling model to ionic solids has been the clarification of the anomalous isotope mass dependence of ionic conduction.[20]

An important equation in the coupling model is the generalized equation for the normalized relaxation function $\Phi(t)$:

$$d\Phi(t)/dt = -W(t)\Phi(t) , \tag{8}$$

where the transition rate $W(t)$ may be time dependent. The time dependence of W has its origin in the coupling between the mobile ions. Interaction between an individual ion with the lattice is usually considered as the cause of the irreversibility of the hopping process of the ion from site to site. As such, the lattice serves as the conventional heat bath. Under certain approximations (the so-called van Hove limit), it has been shown[21] that the interaction of the ion with the heat bath gives rise to a time-independent hopping-relaxation rate W_0 in the hopping-rate equation $d\Phi/dt = -W_0\Phi$. The relaxation rate W_0 is determined by the attempt frequency ν_0 and the microscopic energy barrier. The above equation cannot describe the real situation for systems such as Na β-alumina in which the correlations between mobile ions are known to be important. The coupling model addresses the problem of calculating the effect of the many-body correlations between the relaxing ions on the relaxation rate of an individual ion. This difficult problem is basically concerned with many-body effects in irreversible processes, and an analytical first-principle solution starting from model Hamiltonians, with which $W(t)$ can be calculated explicitly, does not exist at this time. In the absence of an Hamiltonian formalism, we have adopted an alternative nonempirical approach which leads to meaningful results and predictions. Various approaches[8,16–20] have been used to derive the time dependence of the form for $W(t)$. All these have in common the conclusion that the initial relaxation rate W_0 is "slowed down," becomes time dependent and, after a characteristic time ω_c^{-1}, assumes the self-similar time dependence of $W_0(\omega_c t)^{-n}$, i.e.,

$$W(t)=\begin{cases} W_0 & \text{for } \omega_c t < 1 \\ W_0(\omega_c t)^{-n} & \text{for } \omega_c t > 1, \quad 0 < n < 1 . \end{cases} \tag{9}$$

In this way only the functional form of the time dependence of $W(t)$ is deduced and the values of n and ω_c have not been calculated for any real material at this time. Instead, their values can be obtained from experimental data. This model approach can only be successful if it leads to predictions of materials properties which in turn can be verified experimentally. It is interesting to note that the t^{-n} response in Eq. (9) has the same functional dependence as that which was previously reported by Kohlrausch.[22]

Using the relaxation rates $W(t)$ [Eq. (9)] and substituting in Eq. (8), we obtain for $W(t)=W_0$

$$\Phi(t)=\exp[-(t/\tau_0)] \quad \text{for } \omega_c t < 1 , \tag{10}$$

where $\tau_0 = W_0^{-1}$, and for $W(t)=W_0(\omega_c t)^{-n}$

$$\Phi(t)=\exp[-(t/\tau^*)^{1-n}] \quad \text{for } \omega_c t > 1 . \tag{11}$$

Equation (11) has the form of the Kohlrausch fractional-exponential solution, where the relaxation time τ^* is described in terms of the parameters τ_0 and ω_c by

$$\tau^* = [(1-n)\omega_c^n \tau_0]^{1/(1-n)} . \tag{12}$$

There are two important points to be made with regard to Eqs. (9)–(12). First, the expression for τ^* in Eq. (12) is directly related to the quantities ω_c and τ_0 as well as the fractional exponent n. All three quantities (n, ω_c, τ_0) are *determined separately by experiment.* The second point is that there is a direct relationship between the high- and low-frequency response through the microscopic relaxation time τ_0. It is important to note that from the two different time behaviors of the relaxation function $\Phi(t)$ for $t < \omega_c^{-1}$ [Eq. (10)] and for $t > \omega_c^{-1}$ [Eq. (11)], and the requirement of continuity of $\Phi(t)$ at the crossover,[16] a relation similar to Eq. (12) between τ^* in the long-time regime and τ_0 in the short-time regime can be obtained. This represents a simple way to understand the form for Eq. (12).

As defined by Eqs. (10) and (11) the crossover from fractional exponential to the linear exponential is near $t_c = \omega_c^{-1}$. This condition will be defined as "t_c crossover" in time or "ω_c crossover" in frequency. The crossover condition will also depend on the magnitude of the quantity $\omega_c\tau_0$. Thus if the condition $\omega_c\tau_0 \gg 1$ is satisfied (which can be arranged by lowering the temperature, if τ_0 is thermally activated) then it can be shown[19] that $\Phi(t)$ has hardly decayed from unity before it assumes the fractional exponential form of Eq. (11). This property of $\Phi(t)$ is called "fractional-exponential dominance."[16,19] On the other hand, if $\omega_c\tau_0 \ll 1$ then the relaxation function $\Phi(t)$ decays according to the linear-exponential solution from unity to almost zero before its t_c crossover to the fractional-exponential regime. This behavior is called "linear-exponential dominance." There is a "crossover of dominance" when the condition $\omega_c\tau_0 = 1$ is satisfied. The predictive nature of the above formalism distinguishes the present model from recent alternative efforts which have been limited to deducing the Kohlrausch form. Simultaneous application of the coupled relations (10)–(12) to relaxation phenomena in various complex systems has allowed the explanation of additional puz-

zling behavior beyond the Kohlrausch time (or frequency) dependence of the relaxation function Φ. A discussion of specific examples can be found elsewhere.[19,23–27]

IV. RELATIONSHIP CROSSOVER IN Na β-ALUMINA

The coupled-relaxation model will be applied to the data for Na β-alumina which was shown in Figs. 1 and 2. We need to specify the magnitude of the parameters n, ω_c, and τ_0. In addition, we need to examine the possible temperature dependence of these parameters. The fit to M'' in Fig. 1 was obtained for $n=0.64$ and $\log_{10}\tau^*=4.93$ for a temperature $T=113$ K. Equation (12) relates τ^* to the microscopic relaxation time τ_0 which in turn is thermally activated and of the form

$$\tau_0=\tau_\infty \exp(E_a/T) , \tag{13}$$

where the activation energy E_a is in units of K. The best fit to the electric-modulus data has determined that $\tau_\infty=5.6\times10^{-12}$ s and $E_a=810$ K. This value of E_a is in good agreement with the microscopic thermal activation energy of a cation as predicted by Wolf (see Ref. 1 for appropriate references) and as obtained from low-temperature nuclear-magnetic resonance and internal friction measurements.[28–31]

The value of n is temperature dependent, particularly in the range from 100 to 140 K where evidence for structural changes in the Na ion sublattice have been reported.[3,31] Physically, one can view this temperature range as one where the material undergoes a transition from an ionic conductor with liquidlike ionic conductivity at high temperature to a low-temperature glass like phase.[3] The changes in n with temperature are such that n decreases from the 0.64 value at 113 K to 0.55 at 141 K. For $T>141$ K $M^*(\omega)$ data are not available. From an analysis of the temperature dependence[32] of σ_{dc}, to be discussed in Sec. V, we find that $n=0.52$ at 200 K and 0.50 at 300 K.

The final parameter to be specified is ω_c. The choice of $\omega_c=2\pi\times10^{10}$ s^{-1} follows from the observed onset of changes in the 300-K microwave conductivity data in Fig. 2. This value of ω_c must necessarily be considered approximate. As discussed earlier, the marking of ω_c relative to an observed relaxation crossover will depend on the magnitude of the product $\omega_c\tau_0$ and the resulting time dependence of $\Phi(t)$. In Figs. 3 and 4 are shown calculated curves for $\Phi(t)$ using Eqs. (10)–(12) and quoted values for τ_0 at two temperatures (141 and 1200 K). A constant value of $n=0.55$ is chosen in order to illustrate the effect of the variation of $\omega_c\tau_0$. It is apparent from Fig. 3 that the condition $\omega_c\tau_0\gg1$ is satisfied and that the calculated $\Phi(t)$ is close to unity and given by the linear-exponential form until the condition for the t_c crossover has been satisfied. On the other hand, Fig. 4 is appropriate for the condition $\omega_c\tau_0\ll1$. We will show in Sec. V that the predicted crossover defined by the condition $\omega_c\tau=1$ is consistent with dc conductivity data for a value of $\omega_c=2\pi\times10^{10}$ s^{-1}. Thus Fig. 3 ($\omega_c\tau_0\gg1$) is appropriate for describing the ionic conductivity of Na β-alumina at

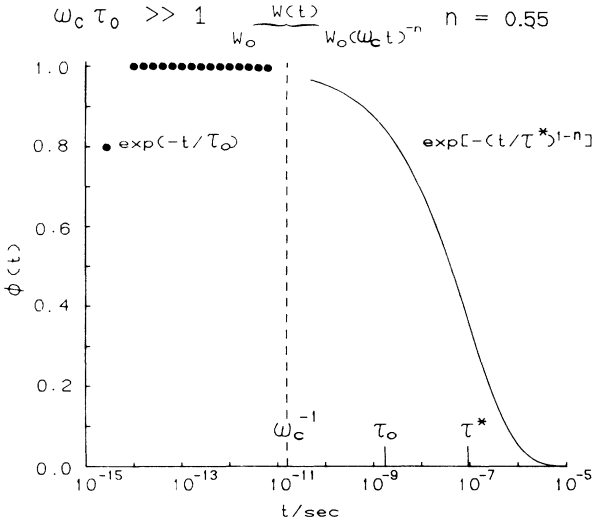

FIG. 3. Sample calculation of the normalized relaxation function $\Phi(t)$ with the choice of $\omega_c=2\pi\times10^{10}$ s^{-1}, $\tau_0=5.6\times10^{-12}\exp[(810\text{ K})/T]$ s at $T=141$ K and $n=0.55$. The effective τ^* calculated according to Eq. (12) is 9.3×10^{-8} s. The t_c crossover from $\exp[-(t/\tau_0)]$ to $\exp[-(t/\tau^*)^{1-n}]$ is shown.

low temperatures (<300 K). For the condition $\omega_c\tau_0\gg1$ it is clear from Eq. (12) that $\tau^*\gg\tau_0$. This implies that it is an excellent approximation to take $\Phi(t)$ to be $\exp[-(t/\tau^*)^{1-n}]$ for all t. In other words, the t_c crossover of $\Phi(t)$ has a negligible effect on the magnitude of $\langle\tau\rangle$. Hence from Eq. (6)

$$\langle\tau\rangle=\int_0^\infty \exp[-(t/\tau^*)^{1-n}]dt$$
$$=[\tau^*/(1-n)]\Gamma[1/(1-n)], \quad \omega_c\tau_0\gg1 \tag{14}$$

and there is a direct relation between the dc conductivity

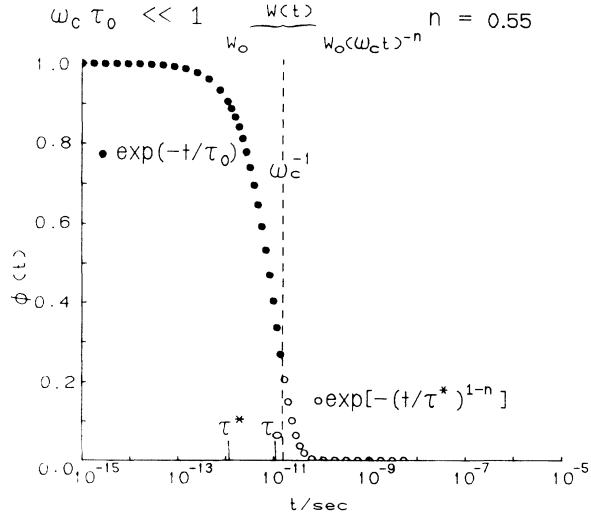

FIG. 4. Sample calculation of the normalized relaxation function $\Phi(t)$ with the choice of $\omega_c=2\pi\times10^{10}$ s^{-1}, $\tau_0=5.6\times10^{-12}\exp[(810\text{ K})/T]$ s at $T=1200$ K and $n=0.55$. The effective τ^* calculated according Eq. (12) is 1.2×10^{-12} s. The condition $\omega_c\tau_0\ll1$ is marginally satisfied and the calculated $\Phi(t)$ is now dominated by $\exp[-(t/\tau_0)]$.

σ_{dc} and τ^* as given by Eq. (5):

$$\sigma_{dc}=(1-n)\epsilon_0/\{M_\infty\Gamma[1/(1-n)]\tau^*\},\quad \omega_c\tau_0\gg 1\ . \tag{15}$$

The last two equations are important for direct comparison between the ac and dc conductivities. In the opposite limit of $\omega_c\tau_0\ll 1$ the domination of $\Phi(t)$ by the fast relaxation $\exp-(t/\tau_0)$ leads to the corresponding relations:

$$\langle\tau\rangle=\int_0^\infty \exp[-t/\tau_0)]dt=\tau_0,\quad \omega_c\tau_0\ll 1 \tag{16}$$

and

$$\sigma_{dc}=\epsilon_0/M_\infty\tau_0,\quad \omega_c\tau_0\ll 1\ . \tag{17}$$

The coupling model can now be applied to calculate the electric modulus and ionic conductivity for values of n, ω_c, and τ_0 which were specified above. Using Eqs. (10)–(12) in conjunction with the definition for M'' and σ in Eqs. (1)–(4) we have calculated $M''(\omega)$ and $\sigma(\omega)$ for three representative temperatures (113, 200, and 300 K). The results of this calculation are shown in Figs. 5 and 6. The overall agreement between these calculated curves and the data shown in Figs. 1 and 2 is quite good. There are some small quantitative differences particularly at 113 K. The primary reason for these discrepancies between model and experiment is the breakdown of the assumption that relaxation due to ionic conduction is the dominant contribution to the dielectric loss. As temperatures fall below ~ 150 K there are significant contributions due to other relaxation mechanisms, including the tunneling motion of ions. These additional contributions, which are especially important at high frequencies, are not explicitly included in the relaxation formalism outlined above. Consequently, the calculated conductivity above 10^{10} Hz for $T=113$ K and to a lesser extent at 200 K underestimates the actual conductivity. For this same reason the electric-modulus-data points above 10^{10} Hz in Fig. 1 lie above the values above 10^{10} Hz predicted by the M'' calculation in Fig. 5.

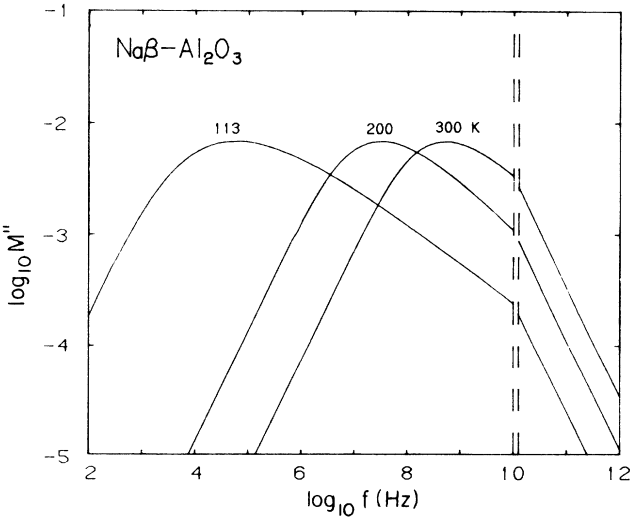

FIG. 5. Calculated imaginary part of the electric modulus $M''(f)$ vs frequency f. Dashed lines indicate $\omega_c\tau=1$. Approach of calculated curves toward $\omega=\omega_c$ is deomonstrated in Fig. 3.

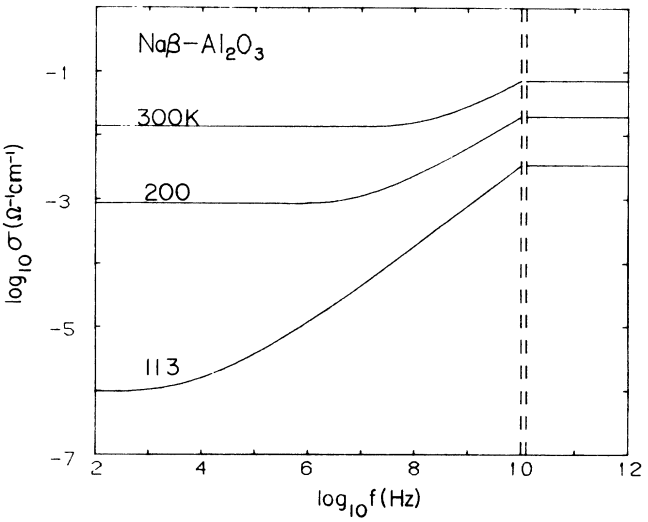

FIG. 6. Calculated ac conductivity. Details are described in text. Significance of dashed lines as in Fig. 5.

It is clear from Fig. 6 that the coupling model can reproduce the significantly different temperature dependences observed for the highest (10^{10}–10^{12} Hz) and lowest ($<10^2$ Hz) frequencies. The temperature dependence at low frequencies approaches that for the well-known dc conductivity, which will be discussed in more detail in the next section. The temperature dependence above 10^{10} Hz has not been explained satisfactorily heretofore. In Fig. 7 are shown previously published data at 9.46 GHz for temperatures between 300 and 635 K. Within experimental error the microwave conductivity is consistent with a temperature-activated form with an activation energy of approximately 810 K, which is the same as E_a defined in Eq. (13). This is precisely the expected activation energy for this regime where the condition $\omega\tau^*\gg 1$ is satisfied. Further discussion on the point of activation energy follows in Sec. V.

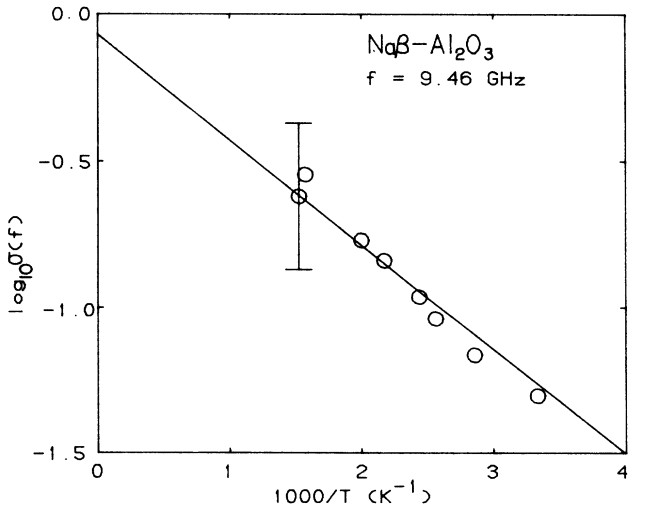

FIG. 7. Arrhenius plot of $\log_{10}\sigma(f)$ vs $1000/T$ for $f=9.46$ GHz and $T>300$ K.

V. dc CONDUCTIVITY: EVIDENCE FOR DOMINANCE CROSSOVER

The general expression for σ_{dc} is given by Eq. (5). The form for $\langle\tau\rangle$ is given by Eqs. (14) and (16) for the limiting cases $\omega_c\tau_0 \gg 1$ and $\omega_c\tau_0 \ll 1$, respectively. If τ_0 is thermally activated as $\tau_0=\tau_\infty \exp(E_a/kT)$, then for $\omega_c\tau_0 \ll 1$, according to Eqs. (5) and (16), σ_{dc} will be thermally activated with activation energy E_a. On the other hand, if $\omega_c\tau_0 \gg 1$, then according to Eqs. (5) and (14) σ_{dc} will be thermally activated with activation energy E_a^* such that

$$\tau^* = \{[1-n(T)]\omega_c^{n(T)}\tau_0\}^{1/[1-n(T)]} \exp(E_a^*/kT) , \quad (18)$$

where

$$E_a^* = E_a/[1-n(T)] \quad (19)$$

and where the temperature dependence of n has been explicitly included. The two different activated regimes as defined by Eqs. (16)–(19) characterize the occurrence of dominance crossover.

The dc conductivity of Na β-alumina has been measured by various investigators with contact[32] as well as contact-free[33] techniques. There is general agreement that if the conductivity is plotted according to the Arrhenius expression $\sigma_{dc}T=\sigma_0^* \exp(-H/RT)$, the plot is linear. In that case the constants H and σ_0^* have the values 3.79 kcal/mole and 2.37×10^3 $(\Omega\,\mathrm{cm})^{-1}$ K, respectively. However, there is strong supportive evidence[34,35] that the more appropriate way to analyze the ionic conductivity is in terms of a simple Arrhenius expression $\sigma_{dc}=\sigma_0 \exp(-H/RT)$. This conclusion is also consistent with the Maxwell relation, Eq. (5), which does not exhibit an explicit temperature factor in the preexponential. Analysis of experimental data of other ionic conductors[4,5,23] reveals the actual temperature dependences of M_∞ and n and lends further support to a temperature-independent prefactor of σ_{dc}. Given the interpretation of the ionic conductivity in terms of the simple Arrhenius formula leads to a plot of $\log\sigma_{dc}$ versus $1/T$ which will no longer be linear. The apparent activation energy defined by $-d\ln\sigma_{dc}/d(1/T)$ can be evaluated from the expression $\sigma_{dc}T=\sigma_0^* \exp(-H/RT)$. Its value, in K, is temperature dependent and given by the equation:

$$-d\ln\sigma_{dc}/d(1/T) = 1908 - T \quad \text{for } 123 < T < 1093 \text{ K} . \quad (20)$$

At the highest temperature of 1093 K, the effective activation energy is equal to 815 K. This value should be identified with E_a provided the condition $\omega_c\tau_0 \ll 1$ is satisfied. The value of τ_0 is calculated using Eq. (17), where $\sigma_{dc}=0.38$ $(\Omega\,\mathrm{cm})^{-1}$ at $T=1093$ K and $M_\infty=0.02$ as taken from low-temperature dielectric-loss data. We find that $\tau_0=1.17\times10^{-11}$ s and with the previously determined value of $\omega_c=2\pi\times10^{10}$ Hz we find that $\omega_c\tau_0=0.73$ at 1093 K. Hence the dominance crossover occurs near the latter temperature and to a very good approximation we can set E_a equal to the activation energy at $T=1093$ K, i.e.,

$$E_a = 810 \text{ K} \quad (\text{or } 0.07 \text{ eV}) . \quad (21)$$

This value together with Eqs. (19) and (20) leads to the relation

$$n(T) = 1 - 810/(1908 - T) . \quad (22)$$

The temperature-dependent values for n predicted by Eq. (22) are $n=(300\text{ K})=0.50$, $n(200\text{ K})=0.53$, $n(141\text{ K})=0.55$, $n(121\text{ K})=0.55$, $n(113\text{ K})=0.55$. These values for $n(T)$ have been used in the calculations shown previously in Figs. 5 and 6. There is good agreement between $n(141\text{ K})$ and the value of 0.53 obtained by fitting the electric-modulus data obtained at 141 K. The discrepancies between the values of $n(T)$ obtained from Eq. (22) and the values obtained previously[3] from fitting the electric-modulus data below 141 K are due in part to structural changes occurring in a broad temperature range around 121 K which are not taken into account in detail in Eq. (22).

Given values of τ_0, ω_c, and $n(T)$, we use Eq. (12) to calculate τ^* as a function of T. Then Eq. (15) leads immediately to the dc conductivity. The solid line in Fig. 8 represents calculations of the dc conductivity for a range of temperatures. The appropriate variables which were chosen were $\omega_c=2\pi\times10^{10}$ s^{-1}, $M_\infty=0.02$, $\tau_0=7\times10^{-12}\exp(810/T)$, and $n(T)$ as given by Eq. (22). All values of these parameters are the same as previously determined except that τ_∞ was modified slightly from 5.6×10^{-12} s to 7.0×10^{-12} in order to achieve an overall better agreement with the experimental measurements given by open squares in Fig. 8. We do not expect exact agreement between predictions and experimental data because $n(T)$ obtained via Eq. (22) is only approximate and any possible temperature dependence of M_∞ has not been taken into account. Considering the uncertainties in these factors, the overall agreement shown in Fig. 8 lends

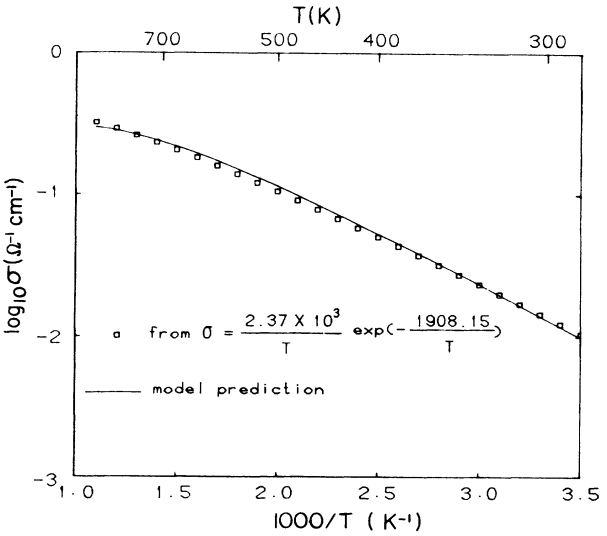

FIG. 8. Plot of dc conductivity vs $1000/T$. The squares are from an equation given by Whittingham and Huggins (Ref. 32) that represents their conductivity measurements very well. The solid line is from the model as described in text.

additional support for the validity of Eq. (8) and can be considered as further evidence for dominance crossover in Na β-alumina.

VI. SUMMARY AND CONCLUSIONS

In this paper we have reexamined the microwave ionic-conductivity data of Na β-alumina for temperatures greater than ~ 100 K where the hopping and not the tunneling motion of ions is expected to dominate the dielectric relaxation. The data exhibit a pronounced change in the frequency dependence of the ac conductivity in the 10^8-10^{10}-Hz range. Below this range the ionic conductivity is frequency dependent and can be modeled very satisfactorily in terms of a fractional-exponential relaxation model, according to which an observable such as an electric field decays as $\exp[-(t/\tau^*)^{1-n}]$, where $0<n<1$. Above 10^{10} Hz the ac ionic conductivity is independent of frequency over at least one decade in frequency, just below the onset of the phonon absorption bands. This observation has been interpreted in this work in terms of the change, or crossover, of the relaxation from a fractional exponential to a simple exponential such as $\exp[-(t/\tau_0)]$. Equation (12) provides a definite relation between the relaxation times τ_0 and τ^* solely in terms of the parameter n and the crossover frequency ω_c. All parameters are directly determined from experiment. For example, a fit to dielectric loss or electric modulus data in the 10^2 to 10^7-Hz range determines n and τ^*. The parameter ω_c can be treated as an adjustable parameter or as determined by the observed distinct change in the frequency dependence of the ac conductivity. In either case we find a consistent fit to all of the dielectric-loss data for a choice of $\omega_c=2\pi\times10^{10}$ s^{-1}. The temperature dependence of τ_0 and τ^* can be directly related to the temperature dependence of the dc and ac conductivities observed for Na β-alumina. The observed relaxation crossover is not expected to be unique to this ionic conductor,[36,37] but is likely to be observed in other disordered electronic or ionic conductors in which the microwave conductivity is not dominated by coupling to phonons.

ACKNOWLEDGEMENT

This work is supported in part by the U.S. Office of Naval Research Contract No. N0001488-WX-24074.

[1]U. Strom, Solid State Ionics **8**, 255 (1983).
[2]D. P. Almond and A. R. West, Solid State Ionics **34**, 73 (1981).
[3]K. L. Ngai and U. Strom, Phys. Rev. B **27**, 6031 (1983).
[4]P. B. Macedo, C. T. Moynihan, and R. A. Bose, Phys. Chem. Glasses **13**, 171 (1972); F. S. Howell, R. A. Bose, P. B. Macedo, and C. T. Moynihan, J. Phys. Chem. **78**, 639 (1974).
[5]C. T. Moynihan, L. P. Boesch, and N. L. Laberge, Phys. Chem. Glasses **14**, 122 (1973).
[6]R. Kohlrausch, Pogg. Ann. Phys. (Leipzig) **12**, 393 (1847).
[7]G. Williams and D. C. Watts, Trans. Faraday Soc. **66**, 800 (1971).
[8]K. L. Ngai, Comments Solid State Phys. **9**, 127 (1979); **9**, 141 (1980).
[9]U. Strom and P. C. Taylor, Phys. Rev. B **16**, 5512 (1977).
[10]U. Strom, *Proceedings of the SPIE Conference on Far Infrared Science and Technology, Quebec, 1986,* edited by J. Rizatt (SPIE, Bellingham, 1986), p. 140.
[11]U. Strom, in *Relaxations in Complex Systems,* edited by K. L. Ngai and G. B. Wright (U.S. GPO, Washington D.C., 1985), p. 229. Available from: National Technical Information Service, U.S. Department of Commerce, 5285 Port Royal Rd., Springfield, VA 22161.
[12]U. Strom, M. von Schickfus, and S. Hunklinger, Phys. Rev. B **25**, 2405 (1982); Phys. Rev. Lett. **41**, 910 (1978).
[13]M. von Schickfus and U. Strom, Phys. Rev. B **28**, 1068 (1983).
[14]V. Provenzano, L. P. Boesch, V. Volterra, C. T. Moynihan, and P. B. Macedo, J. Amer. Ceram. Soc. **55**, 492 (1972).
[15]L. P. Boesch and C. T. Moynihan, J. Noncryst. Solids **17**, 44 (1975).
[16]K. L. Ngai, A. K. Rajagopal, and S. Teitler, Physica **133A**, 213 (1985).
[17]A. K. Rajagopal, S. Teitler, and K. L. Ngai, J. Phys. C **17**, 6611 (1984).
[18]K. L. Ngai, A. K. Rajagopal, R. W. Rendell, and S. Teitler, IEEE Trans. Elect. Insulation **EI-21**, 313 (1986).
[19]K. L. Ngai, R. W. Rendell, A. K. Rajagopal, and S. Teitler, Ann. (N.Y.) Acad. Sci. **484**, 150 (1986).
[20]K. L. Ngai, A. K. Rajagopal, and S. Teitler, J. Chem. Phys. **88**, 5086 (1988).
[21]For a collection of papers see *Stochastic Processes in Chemical Physics,* edited by I. Oppenheim, K. E. Schuler, and G. H. Weiss (MIT Press, Cambridge, MA, 1977).
[22]R. Kohlrausch, Pogg. Ann. Phys. **IV-91**, 56 (1854); **IV-91**, 179 (1854).
[23]K. L. Ngai, R. W. Rendell, and J. Jain, Phys. Rev. B **30**, 2133 (1984).
[24]K. L. Ngai and D. J. Plazek, J. Polym. Sci. Polym. Phys. Ed. **23**, 2159 (1985).
[25]G. B. McKenna, K. L. Ngai, and D. J. Plazek, Polymer **26**, 1651 (1985).
[26]K. L. Ngai and G. Fytas, J. Polym. Sci. Polym. Phys. Ed. **24**, 1683 (1986).
[27]K. L. Ngai and J. Jain, Solid State Ionics **18/19**, 362 (1986).
[28]R. E. Walstedt, R. Dupree, J. P. Remeika, and A. Rodriguez, Phys. Rev. B **15**, 3442 (1977).
[29]M. Villa and J. L. Bjorkstam, Phys. Rev. B **22**, 5033 (1980).
[30]S. G. Greenbaum, U. Strom, and M. Rubinstein, Phys. Rev. B **26**, 5226 (1982).
[31]J. L. Bjorkstam, M. Villa, and G. C. Farrington, Solid State Ionics **5**, 153 (1981).
[32]M. S. Whittingham and R. A. Huggins, J. Chem. Phys. **54**, 414 (1971).
[33]U. Strom and P. C. Taylor, J. Appl. Phys. **50**, 5761 (1979).
[34]R. Syed, D. L. Gavin, and C. T. Moynihan, Commun. Amer. Ceram. Soc. **65**, C-129 (1982).
[35]C. A. Angell, Solid State Ionics **9&10**, 3 (1983).
[36]C. A. Angell and L. M. Torrell, J. Chem. Phys. **78**, 937 (1983).
[37]K. L. Ngai, C. H. Wang, G. Fytas, D. L. Plazek, and D. J. Plazek, J. Chem. Phys. **86**, 4768 (1987).